Thermal and Spectroscopic Studies of Poly(*N*-vinyl pyrrolidone)/Poly(vinyl alcohol) Blend Films

M. H. Abou_Taleb

Physics Department, Faculty of Science, Cairo University, Giza, Egypt

Received 6 April 2007; accepted 19 January 2009
DOI 10.1002/app.30082
Published online 17 June 2009 in Wiley InterScience (www.interscience.wiley.com).

ABSTRACT: Poly(*N*-vinyl pyrrolidone) (PVP) and poly (vinyl alcohol) (PVA) homopolymers and their blended samples with different compositions were prepared using cast technique and subjected to X-ray diffraction (XRD) measurements, infrared (IR) spectroscopy, ultraviolet/visible spectroscopy, and thermogravimetric analysis (TGA). XRD patterns of homopolymers and their blended samples indicated that blending amorphous materials, such as PVP, with semicrystalline polymer, such as PVA, gives rise to an amorphous structure with two halo peaks at positions identical to those found in pure PVP. Identification of structure and assignments of the most evident IR-absorption bands of PVP and PVA as well as their blends in the range 400–2000 cm^{-1} were studied. UV–vis spectra were used to study absorption spectra and estimate the values of absorption edge, E_g, and band tail, E_e, for all samples. Making use of Coats-Redfern relation, thermogravimetric (TG) data allowed the calculation of the values of some thermodynamic parameters, such as activation energy E, entropy $\Delta S^{\#}$, enthalpy ΔH, and free energy of activation $\Delta G^{\#}$ for different decomposition steps in the samples under investigation. © 2009 Wiley Periodicals, Inc. J Appl Polym Sci 114: 1202–1207, 2009

Key words: poly(*N*-vinyl pyrrolidone); poly(vinyl alcohol); IR; optical; entropy; enthalpy

INTRODUCTION

Studies on the thermal and optical properties of polymers have attracted much attention in view of their medical and industrial applications.[1–3] Blending involves physical mixing of polymers, which generates new materials having some of the desired properties of each polymer's component.[4–6] Poly(vinyl alcohol) (PVA) is a well-known water-soluble polymer with high transparency, high flexibility, and has wide commercial applications. Poly(*N*-vinyl pyrrolidone) (PVP) deserves a special attention among the conjugated polymers because of the high environmental stability, easy processability, and moderate thermal conductivity. The optical properties are aimed at achieving better absorption, reflection, interference, and polarization. Thermal measurements reveal the kinetic and thermodynamic parameters of degradation process, which are providing good understanding about the structure change.[7,8] Although the fact that the thermal degradation and optical properties of PVP and PVA homopolymers have been extensively studied,[9–14] a few data reported on PVP/PVA blends from thermal stability and electronic structure point of view.

Hence, in this work, attention has been paid to discuss some thermogravimetric (TG) and optical parameters related to the PVP, PVA homopolymers, and their blends. In addition, X-ray diffraction (XRD) and infrared (IR) spectroscopy were used to reveal the miscibility and the structure change of such blend samples.

EXPERIMENTAL

Both PVP and PVA were purchased by WINLAB Chemicals Ltd. (Leicestershire, UK). Pure polymers and a mixture of PVP and PVA (wt/wt %) were dissolved in double distilled water and stirred overnight at room temperature. The resulting solutions were spread over Teflon sheets and left to dry to form a homogeneous thin film about 100-μm thick. The dried films transferred to vacuum desiccator to ensure good drying. Samples were prepared with the following weight percentages: 100/0, 70/30, 50/50, 30/70, and 0/100 (wt/wt %) PVP/PVA. The nature of the samples films was investigated by means of X-ray diffraction (XRD-BV unit, Philips) using Co Kα radiation generated at 40 kV and 20 mA the range of diffraction angle $2\theta = 4$–40° and the scan rate = 3° min^{-1}. IR absorption measurements were carried out on spectrophotometer (Pye Unicam, Wigan, UK) with a resolution of 4 cm^{-1} in the wavenumber range 2000–400 cm^{-1}. The UV–vis spectra of the thin films recorded by UV–vis

Correspondence to: M. H. Abou_Taleb (mostafamamdou9@hotmail.com).

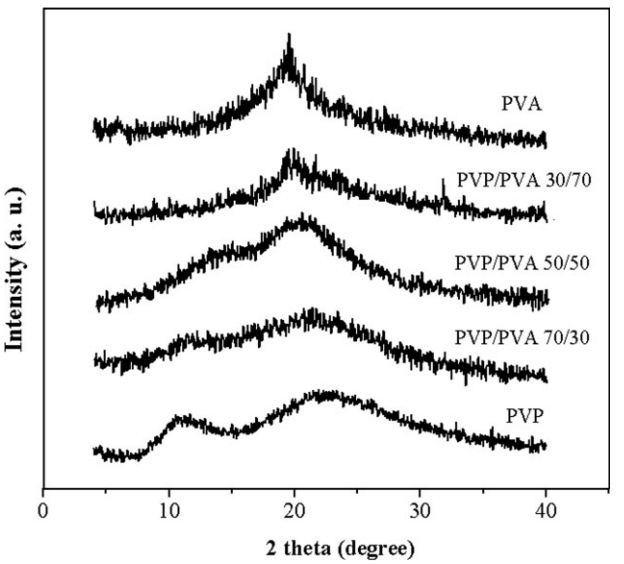

Figure 1 The XRD patterns for PVP and PVA homopolymers and their blends.

spectrophotometer (Perkin–Elmer 4B, Norwalk, CT) at room temperature in the wavelength range 200–800 nm. TGA were carried out by (Shimadzu 50 TGA–50H, Kyoto, Japan) under nitrogen atmosphere. The temperature changes from 50°C to 600°C at heating rate of 10°C min^{-1} with α-alumina as reference material. The TG data were treated in the frame of the Coats-Redfern equations, and the weight losses were determined using the associated TGA-50H software.

RESULTS AND DISCUSSION

XRD diffraction

Figure 1 shows the X-ray patterns for PVP and PVA homopolymers and their blends of composition 70/30, 50/50, and 30/70 (wt/wt %) PVP/PVA. The X-ray of pure PVP film shows amorphous features characterized by two halos centered at $2\theta = 11.5°$ and 22.5°, which are in agreement with published data.[1,8] It is known that glassy amorphous polymers are typically optically clear and show a liquid-like X-ray pattern.[15,16] The X-ray pattern for PVA film shows an intense reflection peak at $2\theta = 19.5°$ diffused in the hollow amorphous region and was assigned to a mixture of (101) and $(10\bar{1})$ reflections.[11,13,17]

The XRD patterns of blend samples of composition 30/70 (wt/wt %) PVP/PVA exhibited the characteristics of pure PVA but with less intense peak. Thus, it is possible to say that the semicrystalline behavior of PVA was decreased on first addition of 30% PVP. Moreover, XRD pattern of blended sample of composition 70/30 (wt/wt %) PVP/PVA shows a weak double broad peak positions identical to that found in pure PVP. As a result, the blends containing PVP $\geq$ 50 wt % show that the semicrystalline structure of PVA is mainly reduced because of the compatibility of the amorphous phase and crystalline phase.[18] For such blends, miscibility between the amorphous components of both homopolymers is possible. Thus, it is promising to suggest that the crystalline form of PVA do not prevent the miscibility between amorphous regions of the polymers in the blended system. The miscibility of PVA/PVP blends was considered as being due to the interactions between the hydroxyl and carbonyl groups of PVA and PVP, respectively.[13]

Infrared spectroscopy

Figure 2 shows the IR absorption spectra of individual polymers and their blends in the wavenumber range from 2000 to 400 cm^{-1}. The main absorption bands of PVP polymer were observed at 1692, 1423, 1374, and 1285 cm^{-1}. These bands were assigned as C=O symmetric stretching, CH_2 bending, O—H bending (in-plane), and C—H deformation respectively.[4,5]

The most remarkable characterizing IR absorption bands of the PVA pure film were detected at 1732, 1428, 1257, 1091, and 847 cm^{-1}. These bands were ascribed as C=O symmetric stretching, CH_2 bending, C—H deformation, C—O stretching, and C—H bending, respectively.[13,19] In the blend samples, the IR spectra show noticeable change in the intensity and shape of some absorption bands, such as the band at 1732 cm^{-1} of PVA overlapped with a band at 1692 cm^{-1} of PVP, which observed as a broadening in the absorption peaks of the blends. This interaction may be due to the miscibility of PVP/PVA blends, which indicates the formation of

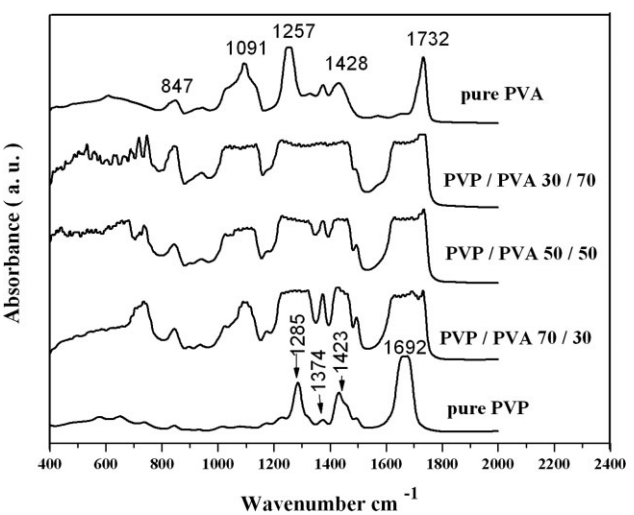

Figure 2 IR absorption spectra for PVP and PVA homopolymers and their blends.

intermolecular hydrogen bond between carbonyl and hydroxyl groups of PVP and PVA polymers, respectively.[14]

Optical properties in UV–vis region

The study of the optical absorption spectra is one of the most productive tools for understanding and developing the band structure and energy gap of both crystalline and amorphous materials.[20,21]

The UV/visible spectra and the relation between the absorbance versus wavelength, in the range between 200 and 800 nm, were recorded for both polymers and their blends (Figures not shown for sake of brevity). The linear absorption coefficient $\alpha(\nu)$ can be directly determined from the optical absorption spectra according to the relation[22]

$$\alpha(\nu) = \frac{1}{d}\ln\left(\frac{1}{T}\right), \quad (1)$$

where T is the transmittance and d is the film thickness. Figure 3 shows the variation of absorption coefficient (α) against incident photon energy ($h\nu$) for virgin polymers (PVP and PVA) and their blends. The relation between $\alpha(\nu)$ and incident photon energy ($h\nu$) exhibit a steep rise near the absorption band edge, and a straight-line relationship is observed at the high α-region as well. The intercept of the extrapolation to zero absorption with photon energy axis was taken as the value of absorption edge E_g. The values of the absorption edge E_g for blend samples are higher than than for individual polymers and increase with increasing the PVA content. This may suggest that there are a certain degree of miscibility in the blends due to the interaction between carbonyl and hydroxyl groups of PVP and PVA polymers, respectively, which was observed as a broadening in the IR absorption band of the blend samples spectra.[23] The absorption edge values E_g obtained are listed in Table I.

TABLE I
The Optical Parameters for PVP and PVA Homopolymers and Their Blend

PVP/PVA (wt/wt %)	E_g (eV)	E_e (eV)
100/0	4.54	0.41
70/30	4.70	0.69
50/50	4.95	0.64
30/70	5.22	0.91
0/100	4.40	3.89

For many amorphous materials, an exponential dependence of absorption coefficient on photon energy was found to obey an empirical relation due to Urbach.[24]

$$\alpha(h\nu) = \alpha_0\left(\exp\frac{(h\nu)}{E_e}\right), \quad (2)$$

where α_0 is a constant and E_e is the width of the tail of the localized states in the band gap.

Figure 4 shows the relation between ln (α) and the incident photon energy ($h\nu$) for individual polymers and their blend samples. The straight lines obtained suggest that the absorption follows the quadratic relation for interband transition[25] and obey the Urbach rule. The values of band tail E_e were calculated from the reciprocal of the slopes of these lines and are listed in Table I. The values of E_e for blend samples are showing irregular variation between those values of pure polymers. The exponential dependence of the absorption coefficient on photon energy in both crystalline and amorphous semiconductors might arise from the random fluctuations of the internal field associated with structure disorder that occurs in many amorphous solids.[26] Tauc[27]

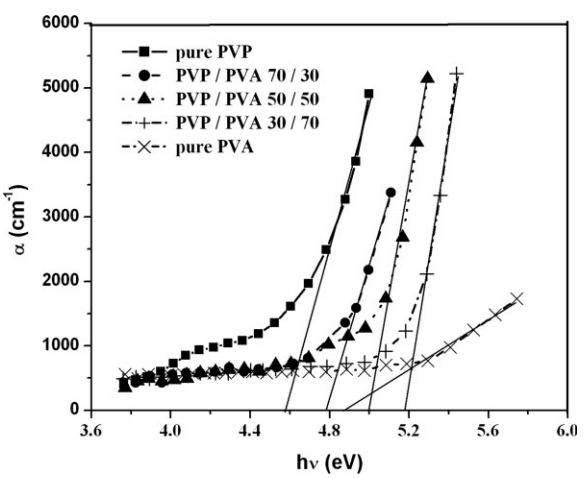

Figure 3 Absorption coefficient (α) as a function of the incident photon energy for PVP and PVA homopolymers and their blends.

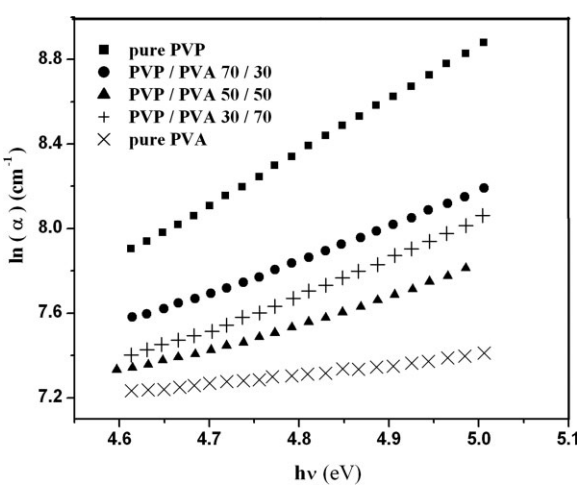

Figure 4 Relation between ln (α) versus the incident photon energy ($h\nu$) for PVP and PVA homopolymers and their blends.

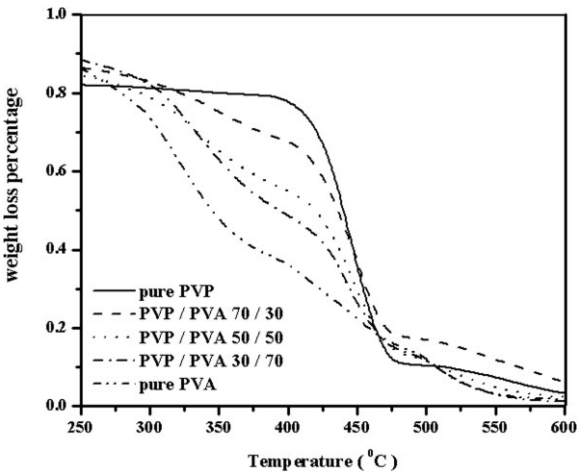

Figure 5 The TG percentage curves for PVP and PVA homopolymers and their blends.

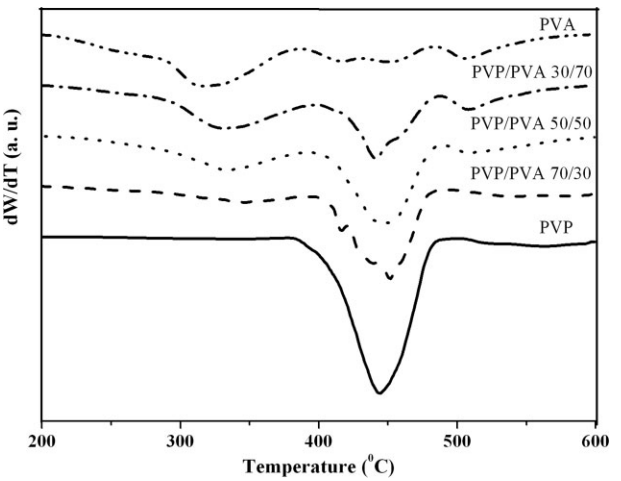

Figure 6 The DTG curves for PVP and PVA homopolymers and their blends.

believed that it takes place from electronic transitions between localized states in the band edge tails, the density of which is assumed to fall off exponentially with energy. In this study, the formation of polymer–polymer blends may induce tails intensity of states by perturbing the band edge via a deformation potential, Coulomb interaction, and fluctuations of internal fields. The values of E_e obtained vary slightly with composition in a regular trend. Thus, the model based on electronic transitions between localized is not preferable.[28]

TG and its derivative

The TG percentage curves and there derivative (DTG) for PVP and PVA homopolymers as well as their blend samples are indicated in Figures 5 and 6, respectively. Peak temperatures for thermal events, T_p, the percentage weight loss, M, residual mass percentage at 600°C, % WL, and the temperature at the end of decomposition, T_e, for the individual polymers and their blends are summarized in Table II. All the studied samples show a small percentage weight loss (10–20%) for the first stage in the temperature range 50–150°C (not included in the present data), which may be attributed to the evaporation of water and/or splitting of monomers. The degradation process of PVP occurs via only one main stage of weight loss after the first one (400–485°C), leading to the formation of esters as a consequence of the scission of the N—C—O bonds at 480°C, confirmed by the evolved NH_3.[29–31] On the other hand, PVA degrades thermally in two stages after the first one. In the PVA second stage (≈ 200–390°C), known as deacetylation, the acetate radicals are generated, which substrates hydrogen from the polymer leading to the formation of polyolefinic backbone. The major recommended reactions occurring in this stage are cis–trans isomerization, aromatization, and crosslinking.[4,13] The presence of second decomposition step in the PVA polymer (in the temperature range 200–390°C) suggests that it has a lower thermal stability compared with PVP polymer. For the third stage (≈ 400–485°C), the structural degradation process of the polyene backbone occurs, leading to the evolution of benzene, toluene, and naphthalene.[4]

The degradation behavior of the PVP/PVA blend films had two main stages of degradation after the

TABLE II
TG and TDG Data for PVP and PVA Homopolymers and Their Blends

	Stage 2			Stage 3			Stage 4			
PVP/PVA	T_p	M	T_e	T_p	M	T_e	T_p	M	T_e	%WL
100/0	–	–	–	446	70	489	–	–	–	3.7
70/30	336	20	361	450	51	484	–	–	–	6.6
50/50	327	31	352	440	43	483	–	–	–	1.4
30/70	323	43	353	438	35	481	503	10	524	3.2
0/100	314	52	370	426	23	468	–	–	–	2.8

T_p: Peak temperature of DTG (in °C).
M: Percentage weight loss (%).
% WL: Percentage weight loss at 600°C.
T_e: Temperature at the end of degradation (in °C).

TABLE III
Thermodynamic Parameters of PVP and PVA Homoplymers and Their Blends

		PVP/PVA (wt/wt %)				
	Stage	100/0	70/30	50/50	30/70	0/100
E (kJ mol^{-1})	S2	–	15.31	23.65	36.06	38.53
	S3	139.4	88.29	68.63	57.69	16.95
	S4	–	–	–	39.66	–
$\Delta S^{\neq}$ (J K^{-1})	S2	–	−31.61	−29.15	−26.28	−17.52
	S3	−30.42	−17.27	−20.60	−22.39	−30.04
	S4	–	–	–	−26.03	–
ΔH (kJ mol^{-1})	S2	–	9.81	18.27	30.63	33.32
	S3	133.01	82.12	62.43	52.27	10.95
	S4	–	–	–	33.09	–
$\Delta G^{\neq}$ (kJ mol^{-1})	S2	–	30.73	37.13	47.79	44.30
	S3	155.07	94.93	77.80	66.89	32.64
	S4	–	–	–	53.68	–

first one. Stages 2 and 3 correspond to the degradation of vinyl acetate (20–43% of weight loss) and vinyl pyrrolidone (35–51% of weight loss), respectively. The results are in agreement with those of the published data.[30] The data describes that PVA suffers deacetylation in the temperature range 200–400°C.[32,33] The degradation process of PVP occurs in the temperature range 400–530°C.[30,34] Blend sample with 30 wt % PVP showed four stages of degradation with the most significant weight loss 43% being observed in Stage 2 (Fig. 6), although 10% weight loss was observed in Stage 4 (Table II). As PVA content increases in the blend samples, the percentage weight loss increases in the Stage 2 whereas it decreases in the Stage 3 as shown in Table II. The TG suggests that the blend 70 wt % PVP is more thermally stable than the individual polymers and their blends 50 and 30 wt % PVP contents, since 70 wt % has a high residual weight percentage at 600°C (Table II).

Table II also shows that the degradation temperatures were shifting to lower values with the increase of the PVA content. Accordingly, the TG and DTG were revealing that the thermal stability of the blend was essentially associated with the VP monomer, losing stability when the percentage of VA in the blend system increases in agreement with the reported results.[30]

Thermodynamic activation parameters of decomposition process were evaluated by making use of the well-known Coats-Redfern relation,[35] nonisothermal kinetic method, in the form

$$\ln\left[\frac{-\ln(1-\delta)}{T^2}\right] = -\frac{E}{RT} + \ln\frac{AR}{\beta E}, \tag{3}$$

where A is a constant, β is the heating rate, R is the universal gas constant, E is the activation energy, and Δ is the fractional weight loss. The plot of $\ln\left[\frac{-\ln(1-\delta)}{T^2}\right]$ against $\frac{1}{T}$ for individual polymers and their blend samples (Figure not shown for sake of brevity) gives a straight line, and the slope of these lines gives the activation energy $\left(-\frac{E}{R}\right)$.

The activation entropy, $\Delta S^{\#}$, the activation enthalpy, ΔH, and free energy of activation, $\Delta G^{\#}$, were calculated using the following equations[36]:

$$\Delta S^{\#} = 2.303\left(\log\frac{Ah}{kT}\right) \tag{4}$$

$$\Delta H = E - RT \tag{5}$$

$$\Delta G^{\#} = \Delta H - T\Delta S^{\#}, \tag{6}$$

where k and h are Boltzmann and Planck constants, respectively, T is the temperature involved in the calculations selected as the temperature at the end of decomposition step, the temperature at which the weight loss is approximately unchanged. The calculated thermodynamic parameters values summarized in Table III. The values $\Delta S^{\#}$, ΔH, and $\Delta G^{\#}$ (Stage 3) for blend samples are decreasing with increasing the PVA content. However, the pronounced deviation of $\Delta S^{\#}$ towards higher values for blend samples compared with individual polymers indicates that the thermal process takes place with significant perturbation of the position order of the macromolecules. In addition, the values of E, $\Delta S^{\#}$, ΔH, and $\Delta G^{\#}$ in the second decomposition step are lower than the values of the third decomposition step. Compared with these results, it can be concluded that the nature of the second decomposition region is orderness, relatively low thermal motion, and relative stability of polyblend system with respect to the third decomposition process.

CONCLUSIONS

The data obtained indicate a high miscibility between different compositions of PVP and PVA due to

electrostatic interactions of polar carbonyl group (C═O) of PVP and hydroxyl group (─OH) of PVA, which are capable of interacting mutually through hydrogen bond. The XRD patterns of blend samples of PVP content $\leq$30 wt % reveal that the semicrystalline structure of PVA is essentially sustained whereas for relatively higher concentration $\geq$50 wt % the two halo amorphous peaks of pure PVP are observed and semicrystalline structure of PVA is mainly destroyed. The increase of absorption edge of the blend samples compared with that of pure PVA may attribute to the decrease of crystallinity induced by mixing with PVP, which was confirmed by XRD data. The energy tail values vary slightly with composition. The thermal stability of the blend samples was enhanced with increasing PVP content. This may attributed to the intermolecular crosslinking reaction, which gives highly compatible impact blend system.

References

1. Razzak, M. T.; Erizal, Z.; Dewi, S. P.; Lely, H.; Taty, E.; Sukirno, S. Radiat Phys Chem 1999, 55, 153.
2. Devi, C. U.; Sharma, A. K.; Rao, V. V. R. N. Mater Lett 2002, 56, 167.
3. Reddy, Ch. V. S.; Sharma, A. K.; Rao, V. V. R. N. J Mater Sci Lett 2002, 21, 105.
4. Cláudia, M. Z.; Oliveira, R. V. B.; Guiotoku, M.; Pires, A. T. N.; Soldi, V. Polym Degrad Stab 2005, 90, 21.
5. Wu, K. H.; Wang, Y. R.; Hwu, W. H. Polym Degrad Stab 2003, 79, 195.
6. Reddy, Ch. V. S.; Han, X.; Zhu, Q. Y.; Mai, L. Q.; Chen, W. Microelectron Eng 2006, 83, 281.
7. Kim, K. J.; Doi, Y.; Abe, H.; Martin, D. P. Polym Degrad Stab 2006, 91, 2333.
8. Liu, H. G.; Lee, Y. I.; Qin, W. P.; Jang, K.; Feng, X. S. Mater Lett 2004, 58, 1677.
9. Yakuphanoglu, F. Opt Mater 2006, 29, 253.
10. Charles, M. W.; Nick, H., Jr.; Gregory, E. S. Physical Properties of Semiconductors; Prentice-Hall: Englewood Cliffs, NJ, 1989.
11. Tawansi, A.; Zidan, H. M.; Oraby, A. H.; Dorgham, M. E. J Phys D: Appl Phys 1998, 31, 3428.
12. Van den Mooter, G.; Wuyts, M.; Blaton, N.; Busson, R.; Grobet, P.; Augustijns, P.; Kinget, R. Eur J Pharm Sci 2001, 12, 261.
13. Jayasekara, R.; Harding, I.; Bowater, I.; Christie, G. B. Y.; Lonergan, G. T. Polym Test 2004, 23, 17.
14. Lewandowska, K. Eur Polym J 2005, 41, 55.
15. Wignall, G. D. Small Angle Neutron and X-Ray Scattering, In Polymer Properties Handbook, 2nd ed.; Mark, J. E., Ed.; Springer Verlag, 2006; p 407.
16. Gedde, U. W. Polymer Physics; Chapman and Hall: London, 1995.
17. Jaworska, N.; Sakurai, K.; Gaudon, P.; Guibal, E. Polym Int 2003, 52, 198.
18. Cheung, Y. W.; Guest, H. J. J Polym Sci Part B: Polym Phys 2000, 38, 2976.
19. Friedlander, H. N.; Hassis, H. E.; Pritchard, J. G. J Polym Sci Part A: Polym Chem 1966, 4, 649.
20. Pol, M.; Hirota, K.; Sakata, H. Physica Status Solidi 2003, 196, 396.
21. Qusrowi, A. F. J Cryst Res Technol 2005, 40, 610.
22. Yakuphanoglua, F.; Sekercib, M.; Evinc, E. Phys B 2006, 382, 21.
23. Yakuphanoglu, F.; Arslan, M.; Küçükislamoğlu, M.; Zengin, M. Sol Energy 2005, 79, 96.
24. Urbach, F. Phys Rev 1953, 92, 1324.
25. Davis, E. A.; Mott, N. F. Philos Mag 1970, 22, 903.
26. Dow, J. D.; Redfield, D. Phys Rev B 1972, 5, 594.
27. Tauc, J.; Zanimi, M. J Non–Cryst Solids 1977, 23, 349.
28. Al Ani, S. K. J.; Hogarth, C. A.; Halawany, R. A. J Mater Sci 1985, 20, 661.
29. Rosiak, J.; Olejniczak, J.; Pekala, W. Radiat Phys Chem 1990, 36, 747.
30. Bianco, G.; Soldi, M. S.; Pinheiro, E. A.; Pires, A. T. N.; Gehlen, M. H.; Soldi, V. Polym Degrad Stab 2003, 80, 567.
31. Shaker, J. A.; Diab, M. A. Polym Degrad Stab 1998, 60, 253.
32. Sivalingam, G.; Karthik, R.; Madras, G. Polym Degrad Stab 2004, 84, 345.
33. McNeill, I. C.; Ahmed, S.; Memetea, L. Polym Degrad Stab 1995, 48, 89.
34. Ishida, H.; Lee, Y. H. Polymer 2001, 42, 6971.
35. Coats, A. W.; Redfern, J. P. Nature 1964, 201, 68.
36. Yakuphanoglua, F.; Gorgulub, A. O.; Cukurovali, A. Phys B 2004, 353, 223.